Received: 31 March 2023 | Revised: 12 May 2023 | Accepted: 31 May 2023

DOI: 10.1002/bit.28466

ARTICLE

BIOTECHNOLOGY AND BIOENGINEERING WILEY

Real-time detection of mAb aggregates in an integrated downstream process

Mariana N. São Pedro[1] | Madelène Isaksson[2] | Joaquín Gomis-Fons[2] | Michel H. M. Eppink[3,4] | Bernt Nilsson[2] | Marcel Ottens[1]

[1]Department of Biotechnology, Delft University of Technology, Delft, The Netherlands

[2]Department of Chemical Engineering, Lund University, Lund, Sweden

[3]Byondis B. V., Nijmegen, The Netherlands

[4]Bioprocessing Engineering, Wageningen University, Wageningen, The Netherlands

Correspondence
Marcel Ottens, Department of Biotechnology, Delft University of Technology, Van der Maasweg 9, Delft 2629 HZ, The Netherlands.
Email: m.ottens@tudelft.nl

Funding information
CODOBIO

Abstract

The implementation of continuous processing in the biopharmaceutical industry is hindered by the scarcity of process analytical technologies (PAT). To monitor and control a continuous process, PAT tools will be crucial to measure real-time product quality attributes such as protein aggregation. Miniaturizing these analytical techniques can increase measurement speed and enable faster decision-making. A fluorescent dye (FD)-based miniaturized sensor has previously been developed: a zigzag microchannel which mixes two streams under 30 s. Bis-ANS and CCVJ, two established FDs, were employed in this micromixer to detect aggregation of the biopharmaceutical monoclonal antibody (mAb). Both FDs were able to robustly detect aggregation levels starting at 2.5%. However, the real-time measurement provided by the microfluidic sensor still needs to be implemented and assessed in an integrated continuous downstream process. In this work, the micromixer is implemented in a lab-scale integrated system for the purification of mAbs, established in an ÄKTA™ unit. A viral inactivation and two polishing steps were reproduced, sending a sample of the product pool after each phase directly to the microfluidic sensor for aggregate detection. An additional UV sensor was connected after the micromixer and an increase in its signal would indicate that aggregates were present in the sample. The at-line miniaturized PAT tool provides a fast aggregation measurement, under 10 min, enabling better process understanding and control.

KEYWORDS

antibody aggregation, continuous biomanufacturing, fluorescent dyes, microfluidic sensor, process analytical technology (PAT)

Abbreviations: Bis-ANS, 4-4-bis-1-phenylamino-8-naphthalene sulfonate; CCVJ, 9-(2-carboxy-2-cyanovinyl)julolidine; ColV, column valve; CQA, critical quality attribute; FD, fluorescent dye; FT, flow through; HMW, high molecular weight; InjV, injection valve; InlS, inlet valve; LOD, limit of detection; LoopV, loop valve; MALS, multi-angle light scattering; OutV, outlet valve; VI, viral inactivation; VV, versatile valve; λ_{em}, emission wavelength; λ_{exc}, excitation wavelength.

1 | INTRODUCTION

A challenge in the implementation of continuous biomanufacturing by the biopharmaceutical industry is the shortage of process analytical technologies (PAT) (Chopda et al., 2021; São Pedro, Silva, et al., 2021). A real-time measurement of certain critical quality attributes (CQAs), such as protein aggregation, is imperative to provide decisive information for subsequent steps and to facilitate process control (Mandenius & Gustavsson, 2015). For the biomanufacturing of monoclonal antibodies (mAbs), the presence of high molecular weight (HMW) species is undesirable (Bansal et al., 2019). With several known aggregation inducing factors being present in the downstream process (Telikepalli et al., 2014; Walchli et al., 2020), a PAT tool capable to detect the formation of these HMW species is essential. Miniaturized biosensors as in-line or on-line PAT tool could speed up the analytical measurement to the required time frame for decision-making. The inherent short operation time, the small sample volume required (in the scale of nL or µL) and the easiness of fabrication are just a few advantages provided by the miniaturization of the analytical technique (São Pedro, Klijn, et al., 2021).

Fluorescent dyes (FD), such as 4-4-bis-1-phenylamino-8-naphthalene sulfonate (Bis-ANS) and 9-(2-carboxy-2-cyanovinyl) julolidine (CCVJ), have been employed to detect and study protein aggregation (Paul et al., 2017). The fluorescence of these molecules is intensified due to changes in the hydrophobicity, Bis-ANS (He et al., 2010), or the viscosity of the surrounding environment, CCVJ (Oshinbolu et al., 2018). Since these dyes provide an immediate and straightforward measurement of aggregation, a FD-based microfluidic biosensor for aggregate detection was designed and developed. A zigzag micromixer, represented in Figure 1, is capable of effectively mixing two different streams within 30 s (São Pedro et al., 2022). The micromixer is comprised of two inlets and one outlet, where the mixing occurs due to the 45° zigzag design, with a total of 30 mixing units. This zigzag structure was applied to detect the presence of HMW species in a variety of mAb aggregation samples, induced by different induction factors (like temperature, freeze-thawing, or low pH incubation). Depending on the FD employed, the developed micromixer was able to robustly detect, at least, 2.5% of aggregation (São Pedro et al., 2023).

Although the micromixer was able to successfully detect aggregation in a single unit operation, an anion exchange (AEX) chromatography (São Pedro et al., 2023), further validation in an integrated downstream process is still required. Therefore, in this work, the developed PAT tool will be assessed for aggregate detection in a lab-scale integrated system, established in an ÄKTA™ Avant unit. The final steps of a mAb purification scheme were carried out: a low-pH viral inactivation (VI) step followed by two polishing steps, a bind-and-elute cation exchange (CEX) and a flow-through (FT) AEX chromatography step. The presence of aggregates in the final purification steps is critical, especially after the polishing steps, since these steps were designed and developed to remove any product related impurities. After each unit operation, a sample of either the FT pool or the eluate was directly sent to the micromixer for aggregate detection. An increase in the UV absorbance would

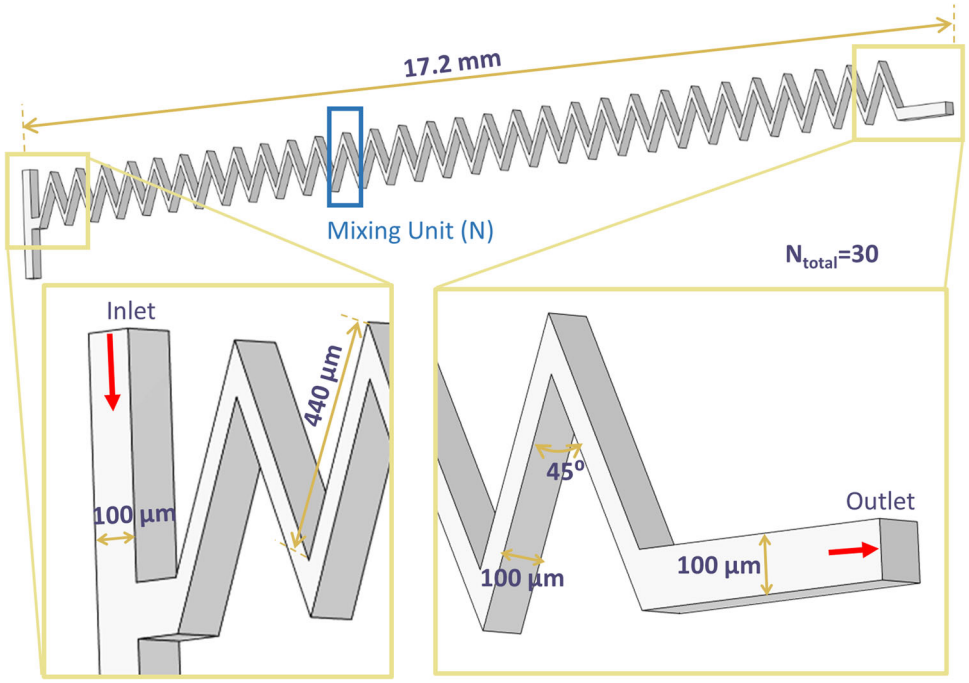

FIGURE 1 3D schematic representation of the micromixer structure, with the relevant measurements described. The zigzag mixing unit (N) of the micromixer is highlighted in blue, with the structure being a consecutive repetition of 30 N and having a total mixing length of around 27 mm (calculated based on the 30 N and the length of the zigzag channel diagonally, 440 µm). The red arrows indicate the flow of both liquids entering in one of the inlets and the resulting mixed liquid exiting at the outlet.

mean that aggregates were present in the sample, which would subsequently be confirmed by off-line analytical size exclusion chromatography (SEC-UPLC). The micromixer was able to effectively detect aggregation in the samples validated with an offline measurement, demonstrating the potential of creating a real-time measurement by the miniaturization of the analytical technique.

2 | MATERIALS AND METHODS

Poly(dimethylsiloxane) (PDMS) was purchased as a Sylgard 184 elastomer kit (Dow Corning). Dimethylsiloxane-(60%–70% ethylene oxide) block copolymer was acquired from Gelest. Sodium phosphate monobasic dehydrate was purchased from Sigma-Aldrich. Di-sodium hydrogen phosphate and sodium chloride were bought from VWR Chemicals (VWR International), whereas sodium acetate was purchased from Merck Aldrich. Acetic acid was obtained from Fluka and sodium hydroxide from J. T. Baker (VWR International). Regarding the FDs, CCVJ, and Bis-ANS were purchased from Sigma-Aldrich and Invitrogen, respectively. The mAb used was supplied by Byondis B. V., with an isoelectric point of 8.6.

The integrated downstream process was implemented in an ÄKTA Avant system (Figure 2), controlled by the software UNICORN™ 7.5 (Cytiva). This ÄKTA unit was equipped with: three pumps (pumps A, B, and sample pump) with inlet valves in each to be able to select different buffers; a column valve (ColV); a loop valve (LoopV); an inlet (InlS) and an outlet (OutV) valve; four versatile valves (VV); an injection valve (InjV); two UV monitors; conductivity and pH sensors; and a 10 mL and two 50 mL superloops™ (all from Cytiva).

2.1 | Sample preparation

The mAb sample was stored in sodium acetate buffer, pH 4.5, at −80°C, in a concentration of 6 mg mL^{-1}. This sample was dialyzed with 50 mM sodium acetate buffer, 100 mM NaCl, pH 5, using amicon ultra-15 centrifugal filters, and concentrated to 40 mg mL^{-1}.

To prepare the stock solutions of the FD dyes, CCVJ was dissolved in dimethyl sulfoxide (Fluka) and Bis-ANS in methanol (Sigma-Aldrich). The exact concentration of each FD stock solution was calculated from the UV absorbance: for CCVJ at 440 nm, with the molar extinction of 25 404 M^{-1} cm^{-1}; and for Bis-ANS at 385 nm, with a molar extinction of 16 790 M^{-1} cm^{-1}. From the stock solutions, the FD solution was diluted with MilliQ water to a concentration of 1 µM for CCVJ and to 0.5 µM for Bis-ANS (São Pedro et al., 2023).

2.2 | Aggregate detection

2.2.1 | Microstructure fabrication

The zigzag micromixer (100 µm high × 100 µm wide × 17.2 mm long) presents two inlets and one outlet (Figure 1). More information on the dimensions and characteristics of the micromixer channel are found in São Pedro et al. (2022). In terms of the structure fabrication, the designed mold was ordered from INESC Microsystems and Nanotechnologies. To reduce the inherent hydrophobicity of PDMS and protein adsorption to the micromixer walls, the structures were fabricated according to Gökaltun et al. (2019). Dimethylsiloxane-(60%–70% ethylene oxide) block copolymer, comprised of poly(ethylene glycol) (PEG) and PDMS segments (PDMS-PEG), were blended with PDMS during device manufacturing, using a 10:1:0.0025 ratio of PDMS, curing agent, and PDMS-PEG. After being degassed, the mixture was poured onto the mold and baked at 70°C overnight. After the PDMS was cured, the chip was removed from the mold and the inlets and outlet were punched in the microstructure. Finally, the PDMS chip was bonded to a glass substrate and sealed with a 20:1 mixture of PDMS to curing agent.

2.2.2 | Off-line analytics

The mAb concentration and level of aggregation was determined off-line by analytical SEC in an UltiMate 3000 UHPLC System (Thermo Fisher Scientific). Five microliters of each sample was injected in an ACQUITY UPLC Protein BEH SEC. 200 Å column (Waters), using the running buffer 100 mM sodium phosphate buffer, pH 6.8. After the sample injection, the flow rate was set to 0.3 mL min^{-1} for 10 min and the protein detection was performed at 280 nm.

2.3 | Integrated downstream process

2.3.1 | Process conditions and buffers

The integrated downstream process included three steps: a low-pH VI; followed by a CEX step in bind/elute mode; and finally an AEX step in FT mode, starting with the injection of 1 mL of mAb sample (concentration of 40 mg mL^{-1}). The VI step was performed at a pH of 3.0 for 60 min, in one of the 50 mL superloop. The CEX column used was a 1 mL HiTrap® Capto™ S ImpAct and the AEX resin was a 1 mL HiTrap® Capto™ Adhere (both obtained from Cytiva). In total, seven different buffers were used for the loading, elution, and stripping of the columns, described in Table 1. The choice of these buffers, as well as the column volumes and flow rates employed, were based on GE Healthcare (2015). Each step was optimized separately and in batch mode beforehand to assess the formation and removal of mAb aggregates. Between several unit operations/steps, the sample buffer conditions had to be adjusted. This was performed through in-line conditioning by dilution. For the VI, the pH of the initial sample had to be lowered from 5.0 to 3.0. A solution of 0.2 M of hydrochloric acid was used, with a dilution ratio of 4:1. To increase the pH after the VI, a 100 mM sodium acetate, 150 mM sodium hydroxide solution was employed, with a dilution ratio of 4:1. Before the AEX column, the CEX eluate was diluted in-line with a ratio of 1:1, with 50 mM sodium

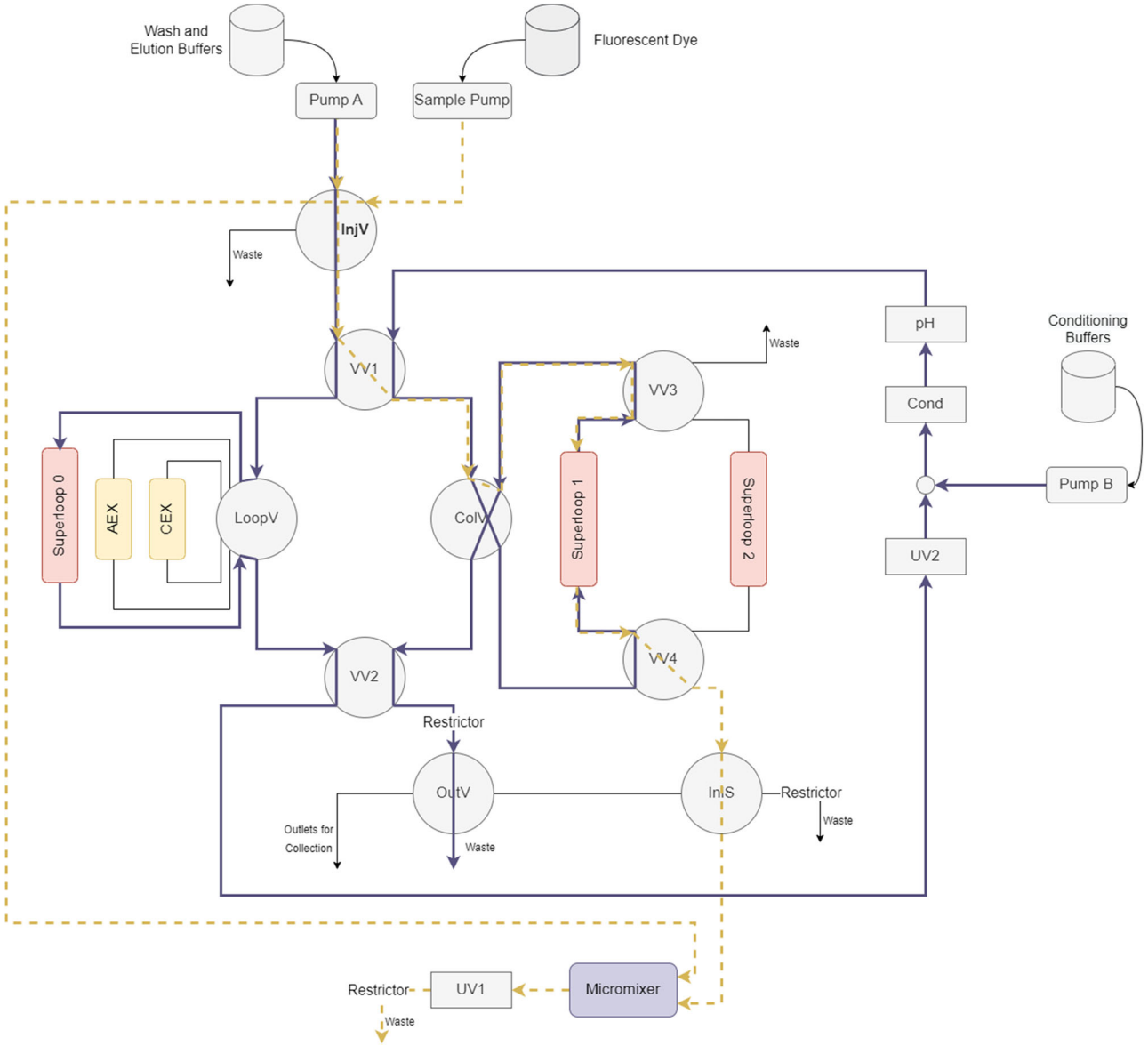

FIGURE 2 Process diagram of the integrated downstream setup with the implementation of the real-time PAT micromixer. The dark blue line represents the flow path for the sample injection in the VI step: Pump A is used to transfer the mAb sample stored in superloop 0, connected to the loop valve (LoopV), to superloop 1, where the VI step occurs, passing through UV2, conductivity (Cond) and pH meter. Since the mAb sample is stored at pH 5, Pump B is used for the in-line sample conditioning to decrease the sample's pH to 3. Similar flow paths are used for the wash and elution of the CEX and AEX chromatography steps, also connected to the LoopV, where the FT or the eluate pools are stored in superloop 1/2. The dashed gold line indicates the flow path used for aggregate detection with the micromixer: the sample pump is used to inject the fluorescent dye into the micromixer through the injection valve (InjV); while, simultaneously, the stored sample in superloop 1 is injected in the micromixer by Pump A. Both streams are mixed in the micromixer structure and the resulting mixed fluid is sent to the UV1 sensor, where, if there is aggregation, an increase in the signal is observed. Black lines represent inactive flow paths. AEX, anion exchange; CEX, cation exchange; FT, flow-through; mAb, monoclonal antibody; PAT, process analytical technologies; VI, viral inactivation.

phosphate solution, pH 6.8. A cleaning-in-place of each column was performed with 1 M NaOH.

2.3.2 | Process setup

The developed system configuration for the implementation of the microfluidic chip in an ÄKTA Avant unit is shown in Figure 2. Pump A was used for the equilibration, elution, and stripping buffers and Pump B was mainly employed for the in-line conditioning buffers. The sample pump was applied to inject the FD into the micromixer structure, passing through the InjV (Figure 2, dashed gold line). The four VVs were used to guide the flow path and to incorporate the two 50 mL superloops in the system. The VI step was performed in superloop 1 (Figure 2, dark blue line). For the remaining process steps, the two superloops independently collected the eluate from

TABLE 1 Buffers used in the integrated downstream set-up experiments.

		Buffer
	Initial sample	50 mM NaOAc + 100 mM NaCl, pH 5.0
VI	Incubation	37.5 mM NaOAc + 75 mM NaCl, pH 3.0
CEX	Equilibration	50 mM NaOAc + 60 mM NaCl, pH 5.0
	Elution	50 mM NaOAc + 240 mM NaCl, pH 5.0
	Stripping	50 mM NaOAc + 500 mM NaCl, pH 5.0
AEX	Equilibration	25 mM NaOAc + 25 mM Na-Pb + 120 mM NaCl, pH 6.2
	Stripping	37.5 mM NaOAc + 75 mM NaCl, pH 3.0

Note: NaOAc corresponds to sodium acetate, Na-Pb to sodium phosphate, and NaCl to sodium chloride.

Abbreviations: AEX, anion exchange; CEX, cation exchange; VI, viral inactivation.

the CEX column, and the FT and the eluate of the AEX column. These samples were shortly stored in superloops 1 or 2 to be later sent to the micromixer channel for aggregate detection. Another particularity of the developed setup was the addition of three different restrictors. By adding these restrictors, the overall process pressure was maintained which was crucial to preserve the integrity of the microfluidic mixer. The LoopV contained the two chromatographic columns and the 10 mL superloop, from where the mAb sample was injected to start the process (superloop 0). The ColV was used as a versatile valve, guiding the flow path and allowing the connection to the two 50 mL superloops. By switching the ColV position, the superloops could either be filled (Figure 2, dark blue line) or emptied (Figure 2, dashed gold line). The OutV was utilized in the sampling of what was collected in the superloop and not further injected in the next step. For example, the FT of the AEX column, that is, the mAb purified product, the stripping of the CEX column and the elution of the AEX column were collected and later analyzed off-line to determine the level of aggregation. The flow paths for remaining phases, such as the CEX column equilibration and elution, are represented in Supporting Information: Figure S1 for a better understanding of the process set-up.

Additionally, two separate UV monitors were employed in this system: UV1, a U9-M monitor able to measure up to three wavelengths; and UV2, a U9-L detector, able to measure only one wavelength. UV1 was placed after the micromixer, to be able to detect aggregation due to the increase in UV absorbance; and UV2, at 280 nm, monitored the chromatographic run, placed after the VV2. The pH and conductivity sensor were also placed after UV2 to monitor the chromatography process.

2.3.3 | Micromixer implementation

The micromixer provides around 90% of mixing efficiency when both streams are simultaneously pumped into the structure at 1 μL min^{-1} (São Pedro et al., 2022). Due to the ÄKTA's inherent pump limitations for lower flows, a flow rate of 3 μL min^{-1} (0.003 mL min^{-1}) was used, which still provided a high mixing efficiency, of around 85%, determined according to São Pedro et al. (2023). With the incorporation of the two 50 mL superloops, this reduction of pump A's flow rate to 3 μL min^{-1} for aggregate detection in the micromixer could be achieved.

To implement the FD-based PAT tool in an ÄKTA unit, several challenges had to be tackled to enable a fast analytical measurement, under 10 min: (1) by placing the micromixer close to the InlS valve (Supporting Information: Figure S2), the volume of the connection tubes, was reduced as much as possible; (2) before the analytical measurement was started, the connection tubes were filled with sample; (3) to clean and remove any remaining sample or FD, the connection tubes and micromixer were flushed with water at a flow rate of 5 μL min^{-1} after each aggregate detection (Supporting Information: Figure S3); and, finally, (4) to eliminate any interference from the FD's intrinsic fluorescence, before the measurement, the UV signal was auto-zeroed with FD and sample buffer in the micromixer. Regarding the wavelengths used in UV1 for aggregate detection, for the FD CCVJ, the selected excitation wavelength (λ_{exc}) was of 435 nm and the emission wavelength (λ_{em}) of 520 nm. For the FD Bis-ANS, the selected λ_{exc} was of 385 nm and the λ_{em} of 520 nm (São Pedro et al., 2023).

2.3.4 | Process control

The ÄKTA systems are normally controlled by the Unicorn software. However, the Unicorn software has several limitations as, for example, operating an ÄKTA system with customized flow paths or introducing process control features. The Orbit software, written in Python, was developed at the department of Chemical Engineering, Lund University. With Orbit, direct communication and control of ÄKTA equipment is enabled via two different protocols (OPC and REST API), and customized control strategies can be implemented, thus overcoming these limitations. In this work, the ÄKTA Avant was controlled via Orbit and a pooling control strategy was implemented: the pooling cut-off times of the collection of the FT and eluate pools of the polishing steps in both 50 mL superloops were based on the UV absorbance at a wavelength of 280 nm, measured on-line by the UV2 monitor (Lofgren et al., 2018). More information on Orbit and how the controller functions can be found in Gomis-Fons et al. (2019) and Löfgren et al. (2021), with several examples on its use described elsewhere (Gomis-Fons, Schwarz, et al., 2020; Moreno-González et al., 2021; Schwarz et al., 2022).

3 | RESULTS AND DISCUSSION

3.1 | Design of the downstream process

To assess the micromixer ability to detect the presence of HMW species in a biomanufacturing process, the final steps of the purification process of mAbs were implemented and integrated in

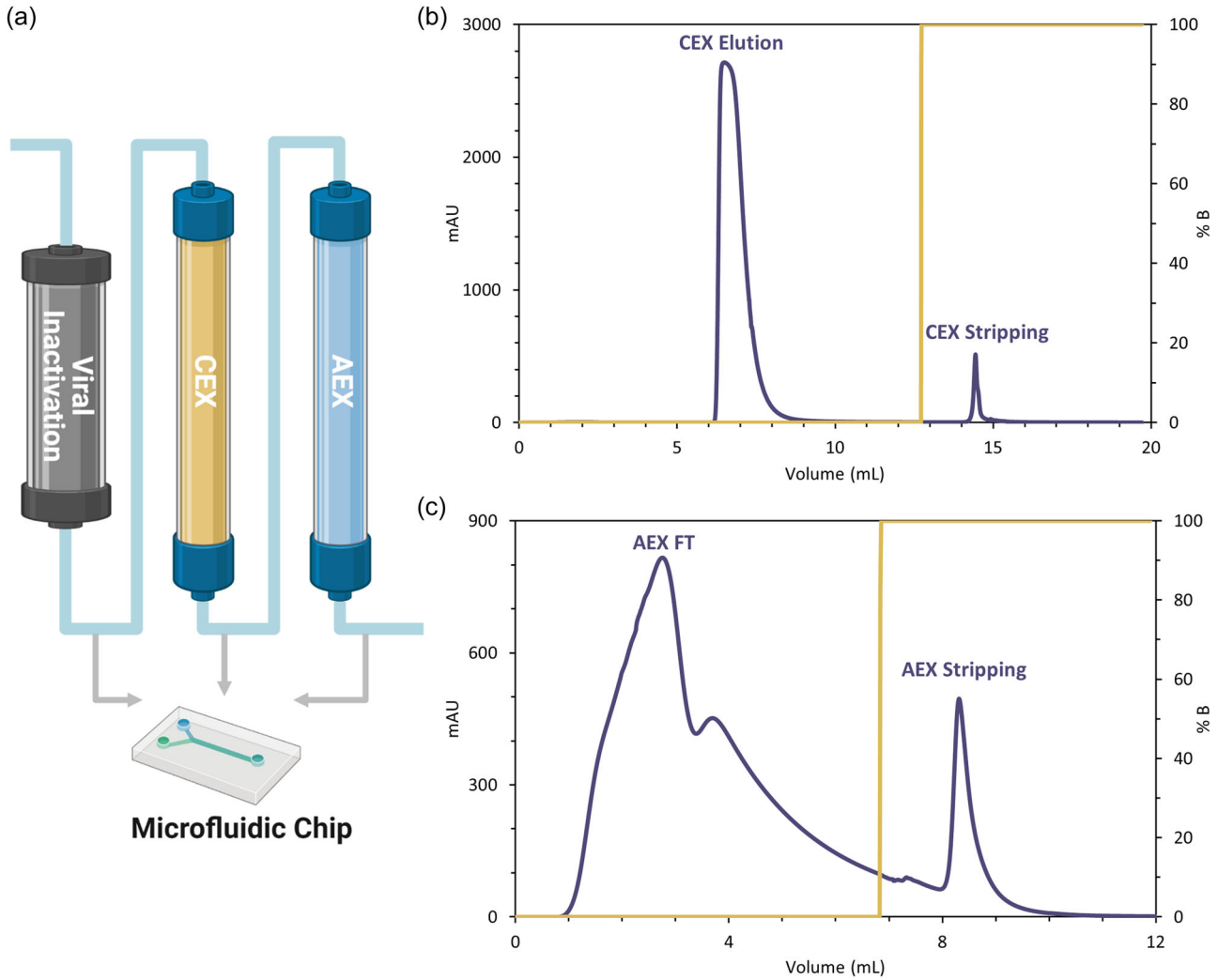

FIGURE 3 (a) Schematic representation of the unit operations implemented in the integrated downstream setup: VI, a CEX, and a AEX chromatography step. A sample of each collected phase is sent directly to the micromixer structure, where mAb aggregation is detected within 10 min. Each unit operation was optimized separately beforehand: first, the mAb sample was incubated at pH 3 for 60 min, and the resulting sample was injected in a (b) CEX column, in a bind-and-elute mode; followed by a (c) AEX step, in a FT mode. The buffers employed can be found in Table 1, the same buffers used in the integrated system. Each sample was also analyzed by SEC-UPLC to determine the aggregation level (Table 2) to confirm aggregate removal within the downstream process. AEX, anion exchange; CEX, cation exchange; FT, flow-through; mAb, monoclonal antibody; SEC, size exclusion chromatography; VI, viral inactivation.

an ÄKTA system. The main goal was to directly send a sample to the micromixer for aggregate detection (Figure 3a). However, the purification steps were first optimized separately and an early assessment of the level of aggregation was performed. Basing the experimental buffers (Table 1) and process conditions on the mAb downstream processes implemented elsewhere (GE Healthcare [2015] and Gomis-Fons, Andersson, et al. [2020]), the three unit operations were reproduced, and the volumes necessary for in-line conditioning were determined. The resulting chromatograms of the bind-and-elute CEX and FT AEX are presented in Figure 3b and c, respectively. The level of aggregation after each unit operation was determined by SEC-UPLC, and is described in Table 2. With the

TABLE 2 Aggregation levels and concentration determined by SEC-UPLC for each collected sample from the batch optimization experiments.

	Aggregation (%)	Concentration (mg mL^{-1})
Initial sample	2.7	36.5
VI incubation	2.8	28.7
CEX stripping	3.2	11.6
AEX FT	0.1	2.0
AEX stripping	13.8	0.4

Abbreviations: AEX, anion exchange; CEX, cation exchange; FT, flow-through; SEC, size exclusion chromatography; VI, viral inactivation.

optimization of each step, the elimination of HMW species was accomplished, with the final mAb product containing merely 0.1% of aggregation. Therefore, the designed integrated process is expected to efficiently remove the aggregates, and the developed PAT tool should only detect aggregation in the VI and the CEX steps, but not in the AEX FT, the final purified product.

3.2 | Implementation of micromixer in the downstream process

The next step was to incorporate and integrate all the steps in an ÄKTA Avant unit, with the implementation of the PAT microfluidic chip (Figure 2, Supporting Information: Figures S1 and S3). Several extra modules were added to a standard ÄKTA unit: a LoopV, four VVs, one extra UV monitor, and three superloops, one of 10 mL and two 50 mL. The function of each additional module is extensively described in Section 2.3.2. The microfluidic chip was operated at a flow rate of 3 µL min^{-1} (0.003 mL min^{-1}), which provided a mixing efficiency of around 85% (São Pedro et al., 2023). Pump A and sample pump inject the sample and the FD into the micromixer, respectively. The incorporation of two superloops in the system was crucial since it allowed to perform not only the VI step, but also to collect the eluate from the CEX column, as well as the FT and the eluate of the AEX column. Thus, the mAb samples could be stored and later directly sent to the micromixer to detect the presence of HMW species (Figure 2, dashed gold line), using a reduced pump A's flow rate. Additionally, with the addition of three restrictors, the system's pressure could be maintained, without the presence of any pressure spikes which could damage the integrity of micromixer or cause the disconnection of the tubes to the micromixer. Thus, a single microfluidic chip could be constantly reused for every measurement performed.

The micromixer was previously validated to successfully detect aggregation in an FT AEX unit operation (São Pedro et al., 2023). However, the detection time, starting with the pumping of the sample to be mixed with the FD and finishing with forwarding the mixed fluid to the UV sensor, took a total of 60 min. Hence, since the micromixer was not able to provide a real-time measurement, a major challenge when integrating this microfluidic sensor was to significantly reduce this detection time. Several design measures and procedures were implemented to decrease this measuring time to merely 10 min, explained in detail in Section 2.3.3. Rathore et al. (2008) used an online-HPLC system to perform pooling of a chromatography column based on product CQAs, like aggregation. The time of analysis in the HPLC was reduced to 11 min, allowing for a real-time decision making for the chromatographic pooling. Therefore, the measuring time of the PAT micromixer was aimed to be reduced to the 10 min mark. Furthermore, to eliminate any interference from the FD's intrinsic fluorescence, the UV signal was auto-zeroed with the injection of FD and the sample buffer in the micromixer before the measurement.

3.3 | Aggregate detection

With the process set up in the ÄKTA system, the final mAb purification steps were reproduced and, after each phase, a sample was directly sent to the developed PAT tool for aggregate detection. First, resorting to the viscosity-sensitive FD CCVJ, a run was performed in the integrated downstream process and the results can be found in Figure 4. The UV signal at 280 nm (dark blue line) was recorded by UV2, controlling the process, whereas the UV signal at 520 nm (dashed gold line) was recorded by UV1. The UV signal at 520 nm was defined to monitor the λ_{em} of the FD CCVJ, meaning that when there was an increase in absorbance, aggregation was present in the analyzed sample. Once more, off-line SEC-UPLC was performed to confirm and determine the level of aggregation of the collected samples which were not loaded into the next purification step (Table 3).

The integrated run started with the cleaning of the micromixer and connection tubes. Afterwards, the mAb sample was injected from the 10 mL superloop 0 to the 50 mL superloop 1, loading the VI step (Figure 2, dark blue line). Since the injection of the mAb sample required the passage through the UV2 detector, the first peak observed at 280 nm in Figure 4 corresponds to this VI loading. During the VI loading, pump B performed sample conditioning by in-line dilution, lowering the mAb pH solution from 5.0 to 3.0. The sample was incubated for 60 min, while the equilibration of the CEX and AEX columns were taking place. After the VI step, a mAb sample was directly sent to the microfluidic sensor for aggregate detection (Figure 2, dashed gold line). A significant increase in the UV absorbance at 520 nm can be observed (Figure 4), which means HMW species are present in the mAb sample. Then, a bind-and-elute CEX was performed, with the eluate also being analyzed in the micromixer. Once again, an increase in the UV signal at 520 nm can be detected, which means that the first polishing step does not completely remove all HMW species present. Subsequently, the CEX eluate was loaded onto the AEX column and the FT was collected for aggregate analysis. Surprisingly, the microfluidic sensor detected HMW species in the AEX FT, that is, the final purified product, which was not expected since the process was optimized for aggregate removal. The off-line analysis by SEC-UPLC revealed that the mAb final product still contained 0.9% of aggregation (Table 3). Hence, the FD CCVJ can detect aggregation in samples containing as low as 1% of HMW species. Nevertheless, aggregate detection using FDs is more related to the properties of the aggregates than actually their amount (Hawe et al., 2008). Therefore, FDs will only provide a qualitative measurement, not quantitative, and an absolute value for its limit of detection (LOD) should not be defined. Later, the AEX column was stripped and the sample pool was sent for aggregate detection and posterior off-line analysis. The micromixer was not able to detect aggregation, which could not be confirmed by the SEC-UPLC analysis since not enough volume was collected. A possible explanation is, since a larger percentage of aggregation was encountered in the mAb product, the absence of a signal in UV1 from the AEX strip sample is due to a poor separation of the HMW

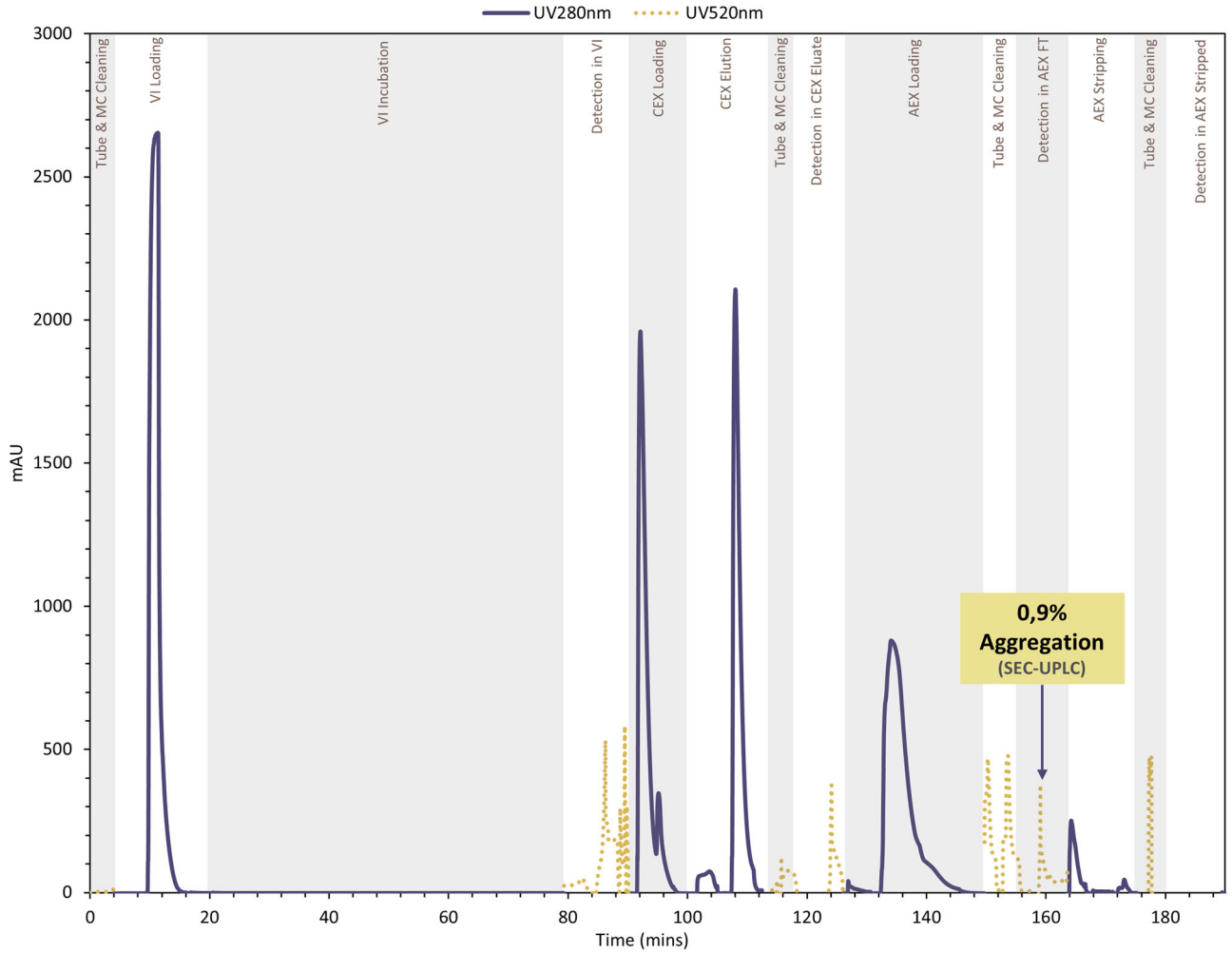

FIGURE 4 Chromatographic profile for a single run in the integrated downstream set-up: VI, CEX, and AEX, with CCVJ ([CCVJ] = 1 μM, λ_{exc} = 435 nm, λ_{em} = 520 nm) as the fluorescent dye (FD) used for detection. The mAb sample ([mAb = 40 mg mL^{-1}) first undergoes the viral inactivation step, where it is incubated at pH 3 for 60 min, followed by CEX in bind-and-elute mode and a FT AEX step. Before each measurement, the micromixer structure is cleaned with water. The UV signal at 280 nm (UV2) is used to monitor the chromatography run whereas the UV signal at 520 nm (UV1) is employed for aggregate detection. The UV1 signal was autozeroed with buffer and FD in the micromixer before each analysis. The examined samples in the microfluidic structure were also analyzed by SEC-UPLC to determine the aggregation level (Table 3). AEX, anion exchange; CEX, cation exchange; FT, flow-through; mAb, monoclonal antibody; VI, viral inactivation.

TABLE 3 Aggregation levels and concentration determined by SEC-UPLC for each collected sample from the integrated downstream runs, for the fluorescent dyes CCVJ ([CCVJ] = 1 μM, λ_{exc} = 435 nm, λ_{em} = 520 nm) and Bis-ANS ([Bis-ANS] = 0.5 μM, λ_{exc} = 380 nm, λ_{em} = 520 nm).

	CCVJ		Bis-ANS	
	Aggregation (%)	Concentration (mg mL^{-1})	Aggregation (%)	Concentration (mg mL^{-1})
Initial sample	4.8	39.3	5.2	40.6
CEX FT	ND	0	ND	0
CEX stripping	32.9	2.4	31.1	3.3
AEX FT	0.9	0.6	0.6	0.6
AEX stripping	-		ND	0

Note: The AEX stripped sample collected was not enough to be analyzed by SEC-UPLC in the CCVJ run. The CEX FT and the AEX Stripping sample for the Bis-ANS run did not contain mAb sample, therefore aggregation was not detected (ND).

Abbreviations: AEX, anion exchange; CEX, cation exchange; FT, flow-through; mAb, monoclonal antibody; SEC, size exclusion chromatography.

species in the final polishing step. Additionally, the AEX strip sample might be too diluted for the FD CCVJ being able to detect aggregation. Since sample collection in each of the superloops is controlled by the UV signal at 280 nm provided by the UV2 monitor, the shortage of volume collected from the stripping of the AEX column already indicated a very diluted sample (Table 3). Nonetheless, the micromixer was successfully implemented and applied, detecting aggregation where HMW species were indeed present during the mAb purification process.

Furthermore, the micromixer sensor was also tested with the hydrophobicity sensitive FD Bis-ANS. The results are described in Figure 5, with the off-line analysis by SEC-UPLC being found in Table 3. An identical process was performed, starting with the VI step and followed by the two polishing steps. Similarly to CCVJ, an increase in the UV signal at 520 nm is observed in the VI and CEX eluate samples. Hence, aggregation was effectively detected by the micromixer once more. However, for the AEX FT, the UV absorbance never increased during the 10 min measuring time. Consequently, aggregation was not detected in the mAb final product, which was later analyzed off-line. The mAb final product contained merely 0.5% of aggregates, which was not detected by the FD Bis-ANS. The regulatory guidelines provided by the United States and the European Pharmacopeia recommend that the mAb final formulation has to be "practically/essentially free" of insoluble aggregates (100 nm to 100 µm), which have been reported to cause immunogenicity (van Beers & Bardor, 2012; den Engelsman et al., 2011). Even though the size of these aggregates would still need to be assessed, 0.5% of aggregation on the final mAb formulation can be considerable acceptable (if the HMW species present are mainly reversible soluble aggregates). Therefore, Bis-ANS can be an ideal choice to be employed in the mAb purification process since it only provides an increase of the UV signal at 520 nm for samples with around 2% of aggregation (São Pedro et al., 2023). Additionally, for the stripping of the AEX column, the micromixer was able to effectively detect aggregation, which was expected (Table 2). Once more, the developed miniaturized PAT tool, using Bis-ANS, successfully detected aggregation in an integrated downstream process. Thus, the FD can be chosen with respect to the maximum recommended

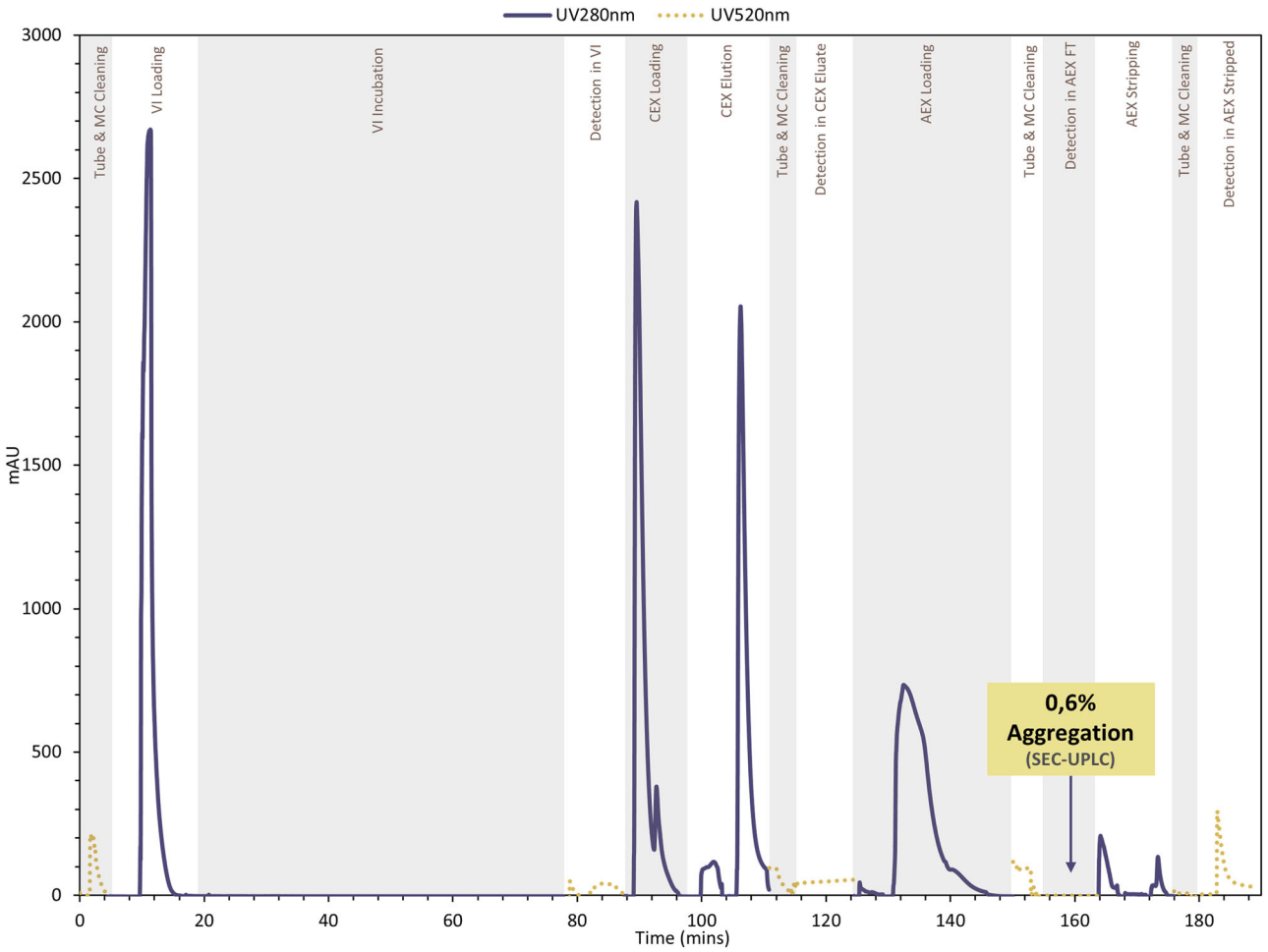

FIGURE 5 Chromatographic profile for a single run in the integrated downstream set-up: VI, CEX, and AEX, with Bis-ANS ([Bis-ANS] = 0.5 µM, λ_{exc} = 380 nm, λ_{em} = 520 nm) as the fluorescent dye used for detection. The same chromatography run was performed as in Figure 4, with the examined samples in the microfluidic structure analyzed by SEC-UPLC to determine the aggregation level (Table 3). AEX, anion exchange; CEX, cation exchange; SEC, size exclusion chromatography; VI, viral inactivation.

concentration of aggregates in the final mAb formulation: the UV signal would only increase if the aggregate level is above the recommended limit.

3.4 | Potential and limitations of the micromixer

The main goal was to develop a PAT tool capable of real-time detection of aggregation in an integrated continuous downstream process. Although the miniaturized PAT tool fulfilled the requirement of detecting the presence of HMW species, this microfluidic sensor cannot be implemented in a truly continuous process. However, the majority of the implemented continuous downstream operations are actually merely semicontinuous, such as the periodic counter current chromatography. The loading of the harvest feed is performed continuously but the washing and elution of the chromatography columns is not, with a discontinuous output of material. Therefore, the developed PAT micromixer could still be easily implemented.

Due to the inherent low flow rates employed in the micromixer, the addition of two superloops was essential to store the product pools. A reduction to lower flow rates, while using the ÄKTA system pumps, could be achieved without jeopardizing the entire purification process. Although the ÄKTA's pumps can technically employ these low flow rates, the entrance of air bubbles could be observed as not enough back pressure was generated. In Figure 4, a sudden increase in the UV signal at 520 nm can be seen at the start of every measurement. The presence of air bubbles result in these oscillations in the UV signal, which might affect the stability of the aggregation measurement. These air bubbles are primarily caused by switching of valve positions and thus flow paths, and the pump's limitation for lower flow rates, making their appearance unavoidable. For example, the sudden peak observed in the tube cleaning before the AEX stripped pool (Figure 4) detection can be attributed to an air bubble. Nevertheless, if the UV signal ends up stabilizing, as seen for the AEX FT pool, the aggregate detection provided by the micromixer is reliable, which was later confirmed by an off-line analysis.

The LOD for this miniaturized PAT tool is directly correlated with the LOD of the FD employed. Depending on the level of aggregation allowed in the final biopharmaceutical formulation, CCVJ and Bis-ANS may be great options to be applied. Recently, several novel FDs have emerged, such as Proteostat, which seems to be better suited to detect small soluble aggregates (Oshinbolu et al., 2018). Hence, the choice of the ideal FD will be critical to produce a reliable aggregate detection and it should be selected according to the needs of removing aggregates in a specific process. Furthermore, even though this work focused on the purification of a biopharmaceutical mAb, these FDs can detect aggregation across a variety of different proteins (Bai et al., 2021; Lindgren et al., 2005; Maarschalkerweerd et al., 2011). Hence, the developed micromixer can be employed in several purification processes where protein aggregation is a CQA.

Unfortunately, a quantification of the degree of aggregation is not yet possible. Since the signal provided by the FD is directly related to the type of aggregate rather than actually its amount, a quantification cannot be achieved (Hawe et al., 2008). For example, in Figure 5, similar UV signals at 520 nm can be observed throughout the process (VI, CEX eluate, and AEX stripped sample), even though the amount of aggregates in each sample differs (Tables 2 and 3). Therefore, this microfluidic sensor is limited to offering a qualitative measurement. For aggregate quantification, the possibility of miniaturizing other analytical techniques should be examined since the developed micromixer demonstrated that its miniaturization produces a real-time measurement. Hydrodynamic chromatography and asymmetrical flow field-flow fractionation (AF4) could be powerful alternatives to be miniaturized and implemented in the developed integrated system (São Pedro, Klijn, et al., 2021).

Nevertheless, the developed PAT tool presents two major advantages when compared to other already reported analytical approaches for a real-time measure of aggregation: the sample volume collected for analysis (30 µL) is negligible, being easily implemented in several biomanufacturing steps; and, since only an extra UV monitor is necessary to perform the analytical measurement, a FD-based microfluidic sensor is a relatively affordable alternative. For example, Patel et al. (2018) created a real-time aggregation measurement by coupling a multi-angle light scattering (MALS) detector to a purification unit. Even though an immediate and in-line measurement is achieved, the cost associated to a MALS detector make this technique not readily available in a biomanufacturing site. Other analytical techniques pose a similar challenge, with an extra and complicated external set-up required to perform the measurement which increases production costs: Raman spectrometry (Yilmaz et al., 2020), near-infrared spectroscopy (Thakur et al., 2020), and light scattering (Rolinger et al., 2020).

4 | CONCLUDING REMARKS

A PAT FD-based microfluidic sensor was successfully implemented in an integrated downstream process, and it was capable of detecting aggregation after each unit operation. First, the final steps in the integrated downstream process for the purification of mAbs, composed of the VI and two polishing steps, were optimized separately for aggregate removal. Then, to implement the previously developed micromixer, an integrated downstream system was developed in an ÄKTA system. A sample was directly sent for aggregate analysis after each step in the purification chain. By adding two superloops and one extra UV sensor, the implementation of the microfluidic sensor was achieved: the two superloops allowed the collection of the mAb samples to be sent for analysis, reducing the flow rate; while the extra UV sensor permitted the monitoring of the chromatographic run while the already existing UV was used for the aggregation measurement. Additionally, several strategies were employed to reduce the measuring time of the microsensor from 60 to 10 min, such as reducing the connection tubes length or filling them with sample/FD beforehand. The microfluidic sensor effectively and robustly detected aggregation when using two distinct FDs, CCVJ, and Bis-ANS, which was later confirmed off-line. Depending on the regulatory

guidelines for the presence of aggregate in the final formulation of the mAb, a more (CCVJ) or less (Bis-ANS) sensitive FD can be selected to detect aggregation in the micromixer.

Although the developed PAT tool cannot produce a quantifiably measurement of the level of aggregation, the microfluidic chip does allow a rapid detection of HMW species. With the implementation in the integrated system, a real-time measurement was achieved, even under the desired 10 min. Therefore, the miniaturization of the analytical technique effectively speeds up the measurement. With the ability to measure real-time CQAs, immediate feedback and control of the process parameters can be achieved. For example, while performing the measurement, a control strategy can be implemented if an increase in the UV signal at 520 nm occurs.

ACKNOWLEDGMENTS

The authors wish to thank the European Union's Horizon 2020 research and innovation programme under the Marie Skłodowska-Curie grant agreement No 812909 CODOBIO, within the Marie Skłodowska-Curie European Training Networks framework.

CONFLICT OF INTEREST STATEMENT

The authors declare no conflict of interest.

DATA AVAILABILITY STATEMENT

The data that support the findings of this study are available from the corresponding author upon reasonable request.

ORCID

Mariana N. São Pedro http://orcid.org/0000-0002-1801-9629
Bernt Nilsson http://orcid.org/0000-0003-3568-7706

REFERENCES

Bai, Y., Wan, W., Huang, Y., Jin, W., Lyu, H., Xia, Q., Dong, X., Gao, Z., & Liu, Y. (2021). Quantitative interrogation of protein co-aggregation using multi-color fluorogenic protein aggregation sensors. *Chemical Science*, *12*(24), 8468–8476. https://doi.org/10.1039/d1sc01122g

Bansal, R., Gupta, S., & Rathore, A. S. (2019). Analytical platform for monitoring aggregation of monoclonal antibody therapeutics. *Pharmaceutical Research*, *36*(11), 152. https://doi.org/10.1007/s11095-019-2690-8

Chopda, V., Gyorgypal, A., Yang, O., Singh, R., Ramachandran, R., Zhang, H., Tsilomelekis, G., Chundawat, S. P. S., & Ierapetritou, M. G. (2021). Recent advances in integrated process analytical techniques, modeling, and control strategies to enable continuous biomanufacturing of monoclonal antibodies. *Journal of Chemical Technology & Biotechnology*, *97*(9), 2317–2335. https://doi.org/10.1002/jctb.6765

den Engelsman, J., Garidel, P., Smulders, R., Koll, H., Smith, B., Bassarab, S., Seidl, A., Hainzl, O., & Jiskoot, W. (2011). Strategies for the assessment of protein aggregates in pharmaceutical biotech product development. *Pharmaceutical Research*, *28*(4), 920–933. https://doi.org/10.1007/s11095-010-0297-1

Gökaltun, A., Kang, Y. B., Yarmush, M. L., Usta, O. B., & Asatekin, A. (2019). Simple surface modification of poly(dimethylsiloxane) via surface segregating smart polymers for biomicrofluidics. *Scientific Reports*, *9*(1), 7377. https://doi.org/10.1038/s41598-019-43625-5

Gomis-Fons, J., Andersson, N., & Nilsson, B. (2020). Optimization study on periodic counter-current chromatography integrated in a monoclonal antibody downstream process. *Journal of Chromatography A*, *1621*, 461055. https://doi.org/10.1016/j.chroma.2020.461055

Gomis-Fons, J., Löfgren, A., Andersson, N., Nilsson, B., Berghard, L., & Wood, S. (2019). Integration of a complete downstream process for the automated lab-scale production of a recombinant protein. *Journal of Biotechnology*, *301*, 45–51. https://doi.org/10.1016/j.jbiotec.2019.05.013

Gomis-Fons, J., Schwarz, H., Zhang, L., Andersson, N., Nilsson, B., Castan, A., Solbrand, A., Stevenson, J., & Chotteau, V. (2020). Model-based design and control of a small-scale integrated continuous end-to-end mAb platform. *Biotechnology Progress*, *36*(4), e2995. https://doi.org/10.1002/btpr.2995

Hawe, A., Friess, W., Sutter, M., & Jiskoot, W. (2008). Online fluorescent dye detection method for the characterization of immunoglobulin G aggregation by size exclusion chromatography and asymmetrical flow field flow fractionation. *Analytical Biochemistry*, *378*(2), 115–122. https://doi.org/10.1016/j.ab.2008.03.050

Healthcare, G. (2015). Continuous chromatography, downstream processing of a monoclonal antibody. 2015 Report 29170800 AA.

He, F., Phan, D. H., Hogan, S., Bailey, R., Becker, G. W., Narhi, L. O., & Razinkov, V. I. (2010). Detection of IgG aggregation by a high throughput method based on extrinsic fluorescence. *Journal of Pharmaceutical Sciences*, *99*(6), 2598–2608. https://doi.org/10.1002/jps.22036

Lindgren, M., Sörgjerd, K., & Hammarström, P. (2005). Detection and characterization of aggregates, prefibrillar amyloidogenic oligomers, and protofibrils using fluorescence spectroscopy. *Biophysical Journal*, *88*(6), 4200–4212. https://doi.org/10.1529/biophysj.104.049700

Löfgren, A., Andersson, N., Sellberg, A., Nilsson, B., Löfgren, M., & Wood, S. (2018). Designing an autonomous integrated downstream sequence from a batch separation process—An industrial case study. *Biotechnology Journal*, *13*(4), 1700691. https://doi.org/10.1002/biot.201700691

Löfgren, A., Gomis-Fons, J., Andersson, N., Nilsson, B., Berghard, L., & Lagerquist Hägglund, C. (2021). An integrated continuous downstream process with real-time control: A case study with periodic countercurrent chromatography and continuous virus inactivation. *Biotechnology and Bioengineering*, *118*(4), 1645–1657. https://doi.org/10.1002/bit.27681

Maarschalkerweerd, A., Wolbink, G.-J., Stapel, S. O., Jiskoot, W., & Hawe, A. (2011). Comparison of analytical methods to detect instability of etanercept during thermal stress testing. *European Journal of Pharmaceutics and Biopharmaceutics*, *78*(2), 213–221. https://doi.org/10.1016/j.ejpb.2011.01.012

Mandenius, C.-F., & Gustavsson, R. (2015). Mini-review: Soft sensors as means for PAT in the manufacture of bio-therapeutics. *Journal of Chemical Technology & Biotechnology*, *90*(2), 215–227. https://doi.org/10.1002/jctb.4477

Moreno-González, M., Keulen, D., Gomis-Fons, J., Gomez, G. L., Nilsson, B., & Ottens, M. (2021). Continuous adsorption in food industry: The recovery of sinapic acid from rapeseed meal extract. *Separation and Purification Technology*, *254*, 117403. https://doi.org/10.1016/j.seppur.2020.117403

Oshinbolu, S., Shah, R., Finka, G., Molloy, M., Uden, M., & Bracewell, D. G. (2018). Evaluation of fluorescent dyes to measure protein aggregation within mammalian cell culture supernatants. *Journal of Chemical Technology & Biotechnology*, *93*(3), 909–917. https://doi.org/10.1002/jctb.5519

Patel, B. A., Gospodarek, A., Larkin, M., Kenrick, S. A., Haverick, M. A., Tugcu, N., Brower, M. A., & Richardson, D. D. (2018). Multi-angle light scattering as a process analytical technology measuring real-time molecular weight for downstream process control. *mAbs*, *10*(7), 1–6. https://doi.org/10.1080/19420862.2018.1505178

Paul, A. J., Bickel, F., Röhm, M., Hospach, L., Halder, B., Rettich, N., Handrick, R., Herold, E. M., Kiefer, H., & Hesse, F. (2017). High-

throughput analysis of sub-visible mAb aggregate particles using automated fluorescence microscopy imaging. *Analytical and Bioanalytical Chemistry*, *409*(17), 4149–4156. https://doi.org/10.1007/s00216-017-0362-2

Rathore, A. S., Yu, M., Yeboah, S., & Sharma, A. (2008). Case study and application of process analytical technology (PAT) towards bioprocessing: Use of on-line high-performance liquid chromatography (HPLC) for making real-time pooling decisions for process chromatography. *Biotechnology and Bioengineering*, *100*(2), 306–316. https://doi.org/10.1002/bit.21759

Rolinger, L., Rüdt, M., Diehm, J., Chow-Hubbertz, J., Heitmann, M., Schleper, S., & Hubbuch, J. (2020). Multi-attribute PAT for UF/DF of proteins-monitoring concentration, particle sizes, and buffer exchange. *Analytical and Bioanalytical Chemistry*, *412*(9), 2123–2136. https://doi.org/10.1007/s00216-019-02318-8

São Pedro, M. N., Eppink, M. H. M., & Ottens, M. (2023). Application of a fluorescent dye-based microfluidic sensor forreal-time detection of mAb aggregates. *Biotechnology Progress*. https://doi.org/10.1002/btpr.3355

São Pedro, M. N., Klijn, M. E., Eppink, M. H. M., & Ottens, M. (2021). Process analytical technique (PAT) miniaturization for monoclonal antibody aggregate detection in continuous downstream processing. *Journal of Chemical Technology & Biotechnology*, *97*(9), 2347–2364. https://doi.org/10.1002/jctb.6920

São Pedro, M. N., Santos, M. S., Eppink, M. H. M., & Ottens, M. (2022). Design of a microfluidic mixer channel: First steps into creating a fluorescent dye-based biosensor for mAb aggregate detection. *Biotechnology Journal*, *18*, 2200332. https://doi.org/10.1002/biot.202200332

São Pedro, M. N., Silva, T. C., Patil, R., & Ottens, M. (2021). White paper on high-throughput process development for integrated continuous biomanufacturing. *Biotechnology and Bioengineering*, *118*(9), 3275–3286. https://doi.org/10.1002/bit.27757

Schwarz, H., Gomis-Fons, J., Isaksson, M., Scheffel, J., Andersson, N., Andersson, A., Castan, A., Solbrand, A., Hober, S., Nilsson, B., & Chotteau, V. (2022). Integrated continuous biomanufacturing on pilot scale for acid-sensitive monoclonal antibodies. *Biotechnology and Bioengineering*, *119*(8), 2152–2166. https://doi.org/10.1002/bit.28120

Telikepalli, S. N., Kumru, O. S., Kalonia, C., Esfandiary, R., Joshi, S. B., Middaugh, C. R., & Volkin, D. B. (2014). Structural characterization of IgG1 mAb aggregates and particles generated under various stress conditions. *Journal of Pharmaceutical Sciences*, *103*(3), 796–809. https://doi.org/10.1002/jps.23839

Thakur, G., Hebbi, V., & Rathore, A. S. (2020). An NIR-based PAT approach for real-time control of loading in Protein A chromatography in continuous manufacturing of monoclonal antibodies. *Biotechnology and Bioengineering*, *117*(3), 673–686. https://doi.org/10.1002/bit.27236

van Beers, M. M. C., & Bardor, M. (2012). Minimizing immunogenicity of biopharmaceuticals by controlling critical quality attributes of proteins. *Biotechnology Journal*, *7*(12), 1473–1484. https://doi.org/10.1002/biot.201200065

Wälchli, R., Ressurreição, M., Vogg, S., Feidl, F., Angelo, J., Xu, X., Ghose, S., Jian Li, Z., Le Saoût, X., Souquet, J., Broly, H., & Morbidelli, M. (2020). Understanding mAb aggregation during low pH viral inactivation and subsequent neutralization. *Biotechnology and Bioengineering*, *117*(3), 687–700. https://doi.org/10.1002/bit.27237

Yilmaz, D., Mehdizadeh, H., Navarro, D., Shehzad, A., O'Connor, M., & McCormick, P. (2020). Application of Raman spectroscopy in monoclonal antibody producing continuous systems for downstream process intensification. *Biotechnology Progress*, *36*(3), e2947. https://doi.org/10.1002/btpr.2947

SUPPORTING INFORMATION

Additional supporting information can be found online in the Supporting Information section at the end of this article.

How to cite this article: São Pedro, M. N., Isaksson, M., Gomis-Fons, J., Eppink, M. H. M., Nilsson, B., & Ottens, M. (2023). Real-time detection of mAb aggregates in an integrated downstream process. *Biotechnology and Bioengineering*, 1–12. https://doi.org/10.1002/bit.28466